DIFFERENTIAL ABSORPTION LIDAR METHOD. CURRENT STATUS OF RESEARCH

V.V. Zuev, M.Yu. Kataev, M.M. Makogon, and A.A. Mitsel'

Institute of Atmospheric Optics,
Siberian Branch of the Russian Academy of Sciences, Tomsk
Received February 13, 1995

This paper summarizes the results of application of differential absorption (DA) method to remote sounding of atmospheric and polluting gases, obtained by different groups of researchers. The lidar systems constructed in the last two decades are reviewed.

1. INTRODUCTION

Laser methods hold a particular place in studies of the gas composition of the atmosphere. Among the advantages of these methods against others for investigating the atmosphere are high spatial and temporal resolution, high speed, and big atmospheric volumes observed. The laser methods give promise since a great variety of interaction phenomena between the electromagnetic radiation and a medium accompany the laser radiation propagation through the atmosphere. Among these phenomena there are light absorption and scattering by atoms and molecules of atmospheric and polluting gases as well as by aerosol particles, resonance and Raman scattering by gas molecules, fluorescence, optical signal distortion due to atmospheric turbulence, etc. Each of these phenomena leads to certain changes in energy, spectral, temporal, and polarization parameters of laser radiation. Recording and interpreting of these changes can yield information practically about all parameters of the atmosphere.[1–7]

About three decades have elapsed since the first publication[8] devoted to the use of a ruby laser for studying the light scattering properties of the atmosphere (1963). During this period a large bulk of data has been obtained, which shows that a great number of conventionally meteorological problems (among them, the estimation of basic meteorological parameters such as air temperature, humidity, pressure, and density) can be solved using laser methods.[1–7,9]

For remote measurements of gas concentrations, air temperature and pressure the following spectroscopic effects are used: resonance absorption, Raman scattering, and fluorescence. Among these effects, the resonance absorption exhibits the largest interaction cross section and, therefore, the laser method based on it is inherently highly sensitive. This method is the subject of the study presented in this paper.

For the first time this method was applied by Schotland.[10] Its idea is that the information about concentration of a gas under study is extracted from the comparison of two lidar signals recorded at two different wavelengths within a sufficiently narrow spectral interval. One wavelength is within an absorption line (band) of the gas under study, whereas another one is out of it. Schotland named this method as differential absorption of scattered energy (DASE). The terms "differential absorption lidar" (DIAL),[11] "differential absorption and scattering" (DAS),[12] or simply "differential absorption" (DA) method[13] are also in common use.

First DIAL measurements were carried out by Schotland, who used the temperature tuning of a ruby laser radiation wavelength at the water vapor absorption line.[10] The ceiling of sounding was 4.3 km. Further development of the DA method allowed the profiles of concentration of such gases as H_2O, NO_2, NO, SO_2, and O_3 to be acquired.[7]

As to the theoretical studies of the DA method, the attention was mainly concentrated on the accuracy characteristics of such laser systems[7,12–15,19] and on the analysis of errors in determination of the profiles of concentration of gases under study from lidar data[16–21] as well as on the development of efficient algorithms for lidar signal processing.[9,15,22,23]

One can find some theoretical and experimental results concerning the DA method in the reviews by Kostko,[24] Kildal and Byer,[25,26] Derr,[27] Grant,[28] as well as in the monographs.[4–7]

The present paper analyzes the current state in studying the differential absorption lidar method as applied to sounding of atmospheric and polluting gases. The lidar systems constructed by different groups of researchers are also reviewed.

2. DIFFERENTIAL ABSORPTION METHOD

The differential absorption lidar method allows the information to be obtained about spatial distribution of a gas under study along a sounding path. Atmospheric aerosol and molecular gases serve as tracers. The mathematical formalism of obtaining the gas concentrations from lidar signals is based on the lidar equation. In a single–scattering approximation it has the form

$$U(\nu_i, R) = \frac{1}{R^2} S_{\text{ins}}(\nu_i)\, S_0(\nu_i, R) \int g(\nu_i - \nu)\, T^2(\nu_i, \nu)\, d\nu\,, \quad (1)$$

where $U(\nu_i, R)$ is an echo–signal from a distance R at a frequency ν_i, $g(\nu_i - \nu)$ is the spectral distribution of laser radiation energy over a pulse, $S_0(\nu_i, R)$ is an optical function of the lidar equation, which is governed by scattering properties of a medium, and $S_{\text{ins}}(\nu_i)$ is an instrumental constant, which has the following form:

for analog mode of recording

$$S_{\text{ins}}(\nu_i) = P_0(\nu_i)\, A\, F\, q_t\, q_r\, (1 - q_l)\, \frac{c\tau}{2}\, \eta\,, \quad (2)$$

and for photon counting mode of recording

$$S(\nu_i) = \frac{E_0(\nu_i)}{h\, c\, \nu_i}\, A\, F\, q_t\, q_r\, (1 - q_l)\, \frac{c(\tau_d + \tau)}{2}\, \eta\,. \quad (3)$$

Here $P_0(\nu_i)$ is the power of a laser transmitter; A is the area of a receiving telescope; q_t and q_r are the efficiencies of the transmitting and receiving optics; F is the geometrical factor

0235-6880/95/08 590-19 $02.00 © 1995 Institute of Atmospheric Optics

(hereinafter it is taken to be unity); q_l is the radiation losses due to ignored factors (for example, incomplete use of the area of a receiving telescope, signal losses in optical elements introduced to equalize dynamic range of signals at wavelengths λ_{on} and λ_{off}, etc.); τ is the pulse duration; τ_d is the strobe duration; $E_0(\nu_i)$ is the radiation pulse energy; $h\,c\,\nu_i$ is the photon energy; and, η is the quantum efficiency of a PMT. The term $T^2(\nu, R)$ in Eq. (1) is

$$T^2(\nu, R) = \exp\left(-2\int_0^R K(\nu, z)\,\rho(z)\,dz\right),$$

where $\rho(z)$ is the gas concentration sought, and $K(\nu, z)$ is the monochromatic absorption coefficient of a gas under study.

Dimensionality of echo–signal depends on the operation mode of a lidar receiving system. When not very distant objects are sounded, signals are usually recorded in analog mode. For this mode $U(\nu_i, R)$ is expressed via instantaneous signal power at a detector output. Weak signals coming from remote volumes are recorded in the photon counting mode. In this case $U(\nu_i, R)$ is the number of single electron pulses at the output of the recording system.

The value $c(\tau_d + \tau)/2 \approx c\,\tau_d/2 = \Delta R$ governs the spatial resolution ($2\Delta R$ is the strobe length) of a signal recorded in a photon counting mode. For analog mode the threshold value of spatial resolution is determined by the laser pulse length, $c\tau/2$.

By sounding of the atmosphere with radiation pulses at two wavelengths, one falling on the absorption line (λ_{on}) and another off it (λ_{off}), and recording echo–signals $U(\lambda_{on}, R)$ and $U(\lambda_{off}, R)$, we can find the gas concentration from the equation

$$\rho(z) = \frac{1}{2\,\tilde{K}_{eff}(\bar{R})\Delta R}\ln\left[\frac{U(\lambda_{off}, R+\Delta R)\,U(\lambda_{on}, R)}{U(\lambda_{on}, R+\Delta R)\,U(\lambda_{off}, R)}\right], \quad (4)$$

where $\tilde{K}_{eff}(\bar{R}) = \tilde{K}_{on}(\bar{R}) - \tilde{K}_{off}(\bar{R})$ is the effective differential absorption coefficient averaged over radiation spectrum and spatial variable within the layer ΔK.

If we consider the signals $U(\lambda_{on}, R)$ and $U(\lambda_{off}, R)$ as continuous functions of the range R, we can write the following expression, instead of Eq. (4):

$$\rho(R) = \frac{1}{2\,\tilde{K}_{eff}(R)}\frac{d}{dR}\ln\left(\frac{U_{off}(R)}{U_{on}(R)}\right) = \frac{\alpha_{exp}(R)}{2\,\tilde{K}_{eff}(R)}; \quad (5)$$

$$\tilde{K}_{eff}(R) = \tilde{K}_{on}(R) - \tilde{K}_{off}(R); \quad (6)$$

$$\tilde{K}_i(R) = \frac{\int g(\nu-\nu_i)\,K(\nu, R)\,T^2(\nu, R)\,d\nu}{\int g(\nu-\nu_i)\,T^2(\nu, R)\,d\nu}, \quad i = \text{on, off}. \quad (7)$$

In the UV spectral range absorption coefficients are slightly structured (for such molecules as ozone, SO_2, NO_2, etc.) and within the laser pulse width they are practically constant. Therefore, effective absorption coefficient $\tilde{K}_{eff} \to \bar{K}_{eff} = \bar{K}_{on} - \bar{K}_{off}$, i.e., it is equal to differential absorption coefficient itself.

3. ERROR IN GAS CONCENTRATION DETERMINED FROM LIDAR DATA

The classical equation for relative error $\delta\rho$ in gas concentration measured with the DA method has the form

$$\delta\rho = \frac{1}{2\,\tilde{K}_{eff}\,r\,\Delta R}\left\{\frac{2}{n}(\gamma_{on}^2 + \gamma_{off}^2) + \gamma_s^2\right\}^{1/2}, \quad (8)$$

where n is the number of radiation pulses, γ_{on} and γ_{off} are random errors in recorded signals U_{on} and U_{off} determined by the signal shot noise, background illumination, and dark current. They are equal to

– for photon counting mode

$$\gamma_i^2 = \frac{N_i + N_b + N_D}{N_i^2}, \qquad i = \text{on, off}, \quad (9)$$

– and for current mode

$$\gamma_i^2 = \frac{2B(P_i + P_b)\,h c\nu_i + \eta^2\,NEP^2}{P_i^2}, \quad (10)$$

where N_i, N_b, and N_D are the numbers of photoelectrons of echo–signals at the wavelength λ_i, background illumination, and dark current, respectively; P_i and P_b are the power of echo–signal at the wavelength λ_i and background illumination; NEP is the noise equivalent power; and $2B$ is the detector frequency bandwidth.

Signals due to background radiation and dark current are equal to

$$N_b = N\frac{1}{hc\nu}A\,q_r\,\Delta\lambda\,\Omega\,\eta\,\tau_d; \quad (11)$$

$$N_D = \left[\frac{NEP}{h\,c\,\nu}\eta\right]^2\tau_d, \quad (12)$$

where $\Delta\lambda$ is spectral width of the filter transmission curve, and Ω is the solid angle of a receiving system field of view.

In Eq. (8) γ_s determines the systematic error, independent of the detector noise. Expression for γ_s has the following form[21]:

$$\gamma_s^2 = 2(\delta_{\beta a}^2 + \delta_{\beta m}^2)\left[\frac{\beta_{off}^a\,\beta_{on}^m - \beta_{on}^a\,\beta_{off}^m}{\beta_{on}\,\beta_{off}}\right] +$$

$$+ (2\,\Delta R)^2\left[(\alpha_{on}^a - \alpha_{off}^a)^2\,\delta_{aa}^2 + (\alpha_{on}^m - \alpha_{off}^m)\,\delta_{am}^2\right] +$$

$$+ (2\,\Delta R)^2\sum_{j=1}^{M}[\tilde{K}_j^2\,\sigma_{\rho j}^2 + \sigma_{K\,j}^2\,\rho_j^2] + (2\,\tilde{K}_{eff}\,\rho\,\Delta R)^2\,\delta_K^2, \quad (13)$$

where $\beta_{on,\,off} = \beta_{on,\,off}^2 + \beta_{on,\,off}^m$.

First two terms in Eq. (13) are connected with the variation of the medium scattering properties occurring during the wavelength tuning. These terms must be taken into account when sounding ozone in the UV.[21] The third term must be taken into account at the presence of interfering gases. Here δ_{ba} and δ_{bm} are relative errors in aerosol and molecular backscattering coefficients, δ_{aa} and δ_{am} are relative errors in extinction coefficient due to aerosol and molecular scattering; $\sigma_{\rho j}$ and σ_{Kj} are errors in concentration and absorption coefficient assigned to the jth interfering gas; K_j is the differential absorption coefficient of the jth interfering gas. When isolated absorption lines are used, the first three terms may be omitted.

Let us consider the fourth term. The relative error in the differential absorption coefficient, δ_K, enters into it. Let us list the main sources of this error.

a. Nonmonochromaticity of laser radiation. Often the monochromatic differential absorption coefficient, K_{eff}, is substituted into Eq. (5) for $\tilde{K}_{\text{eff}}$. As we noted above, it is true only for the UV spectral range. As is seen in Eq. (6), $\tilde{K}_{\text{eff}}$ depends on the shape and width of the laser radiation line $g(\nu_i - \nu)$. The wider is the spectrum of radiation, the greater is the discrepancy between $\tilde{K}_{\text{eff}}$ and K_{eff}. In this case $\tilde{K}_{\text{eff}}$ becomes dependent on the gas concentration sought, $\rho(R)$ (via the square transmittance $T^2(\nu, R)$). This problem was studied in detail in Ref. 20. Here we should like only to note that the error in gas concentration determined from lidar data can reach 40% and even more if the width of laser radiation spectrum is equal to a half–width of the absorption line.

b. Instability of radiation frequency. The absorption coefficient K_{on} is *a priori* given for the frequency ν_{on} (for simplicity we believe that $K_{\text{on}} \gg K_{\text{off}}$). If the radiation frequency is unknown or randomly changing, the error arises in K_{on} obtained. Fortunately, the nonmonochromaticity and instability of laser radiation compensate each other (i.e., the wider is the spectrum of radiation, the smaller is the effect of instability on the absorption coefficient). Nevertheless, the instability in the radiation frequency can result in an error in gas concentration up to 30% (Refs. 15 and 16) when sounding is conducted with a ground based lidar and up to 40% when sounding with a spaceborne lidar.

c. Spectral noise in laser pulse. Narrowing of laser radiation line in tunable, especially, dye lasers very often requires the use of a multicascade generator–amplifier scheme to provide for a required power of sounding radiation. In this case the wide–band radiation of spontaneous emission being amplified takes the features similar to laser radiation (ASE). If the lidar echo–signal and backscattered atmospheric signal from ASE fail to be separated spectrally, then the error arises in interpretation of such lidar data, which can be expressed through the error in absorption coefficient δ_K:

$$\delta_K = \frac{1 - \varepsilon}{1 - \varepsilon + \varepsilon \exp\left\{-2 \int \tilde{K}_{\text{eff}}(z)\, \rho(z)\, dz\right\}}, \qquad (14)$$

where $\tilde{K}_{\text{eff}}$ is the effective differential absorption coefficient, and ε is the degree of "spectral purity" of a signal. This problem was studied in detail in Ref. 19. For $\varepsilon = 0.95$ the value of δ_K is more than 20% at first kilometers along a sounding path. Our calculations show that the error of sounding humidity in the boundary atmospheric layer with a spaceborne lidar can reach 100% for $\varepsilon = 0.99$.

The above listed errors are directly connected with the parameters of a lidar system and they can be classified as the instrumental errors. The distortion of lidar signals by the photorecording instrumentation which will be discussed in the following section also falls into the category of the instrumental errors. Here we should like to note two types of errors, the source of which is the atmosphere itself.

d. Error due to a shift of the absorption line center by air pressure. The influence of this phenomenon is most essential for vertical sounding paths. The measurements[29] of H_2O molecule spectral line profile at 694.38 nm carried out with two PA spectrometers at the pressure of humid air of 1013 mbar and 6.67 mbar allowed the line shift to be determined, which was 0.017 cm^{-1} atm^{-1}. The influence of line shift on the accuracy of determination of water vapor concentration from lidar data is illustrated in Fig. 1. As is seen from Fig. 1, the error can reach 26% at 15 km altitude when sounding with a ground–based lidar (curve *1*). However, the influence of this effect can be weakened if λ_{on} is chosen already shifted by $\delta_{\text{od}} = 0.017$ cm^{-1} from the center of the absorption line (curve *2*).

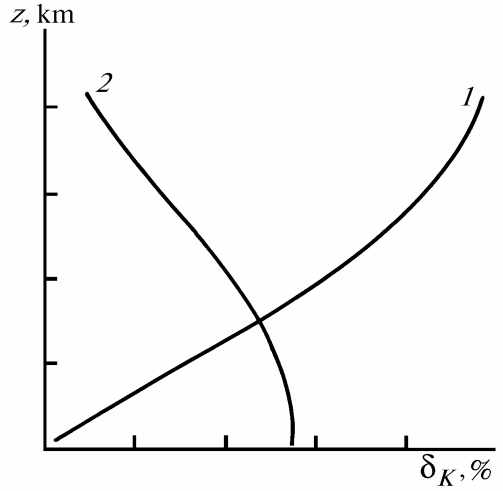

FIG. 1. Error in determination of the absorption coefficient of H_2O *molecule because of neglecting absorption line shift by air pressure at resonance tuning of the laser radiation line at an absorption line; P =* 1 *(1) and* 0.01 atm *(2).*

e. Error due to Doppler broadening of Rayleigh backscattering line. Laser pulse spectrum distortion due to Doppler broadening of Rayleigh backscattering line results in the change of the value of the effective differential absorption, what in its turn leads to the error in determination of the gas concentration. This effect was considered in a number of papers.[19,30–36] Our investigations have shown that this effect is different for two different types of sounding paths, i.e., downward and upward looking paths. The strongest distortions of the results of lidar data interpretation occur in sounding air humidity with a ground based lidar at the altitudes above 10 km. In this case error can reach 100% and more to the point of appearance of negative values, which are physically meaningless, that calls into question the applicability of differential technique of sounding of stratospheric humidity with a ground–based lidar. In sounding with an airborne lidar, the error due to Doppler broadening of Rayleigh backscattering line is less than 16%.

4. NONLINEAR DISTORTIONS OF LIDAR SIGNALS AND WAYS TO CORRECT FOR THEM

Only few papers devoted to study of nonlinear distortions of lidar signals at their recording and the ways of correcting the effects from them can be found in the literature. Mainly the papers deal with the lidars using PMTs as photodetectors. Nonlinear distortions of an output signal from a PMT are caused by internal and external factors, as well as by the effect of a signal recorded on the parameters of a PMT and a photorecorder as a whole. Among the internal factors there are slow and fast changes

of photoemission properties of dynodes, their inhomogeneity, lag, and so on, whereas the ambient temperature, level of distorting background radiation, including the optical one, other radiations, and so on fall into the category of the external factors.

We consider here three distorting factors. The first is connected with the finite capacity of a single–electron pulse (SEP) counter. As a consequence, some pulses remain uncounted.[37]

The second factor is connected with the appearance of false afterpulses. The influence of PMT afterpulsing is seen, as a rule, at the tail of a lidar signal from a distant layers along a sounding path in the form of accumulated excess of recorded output signal over a true lidar signal. The PMT afterpulses appear usually with a time delay of 100 ns after the beginning of PMT photocathode illumination. In the case when a PMT can be considered as a linear system with constant parameters, the recorded lidar signal $U(t)$ distorted by a PMT afterpulsing can be presented in the form of a convolution of an actual signal $\bar{U}(t)$ arriving at the PMT's photocathode with the PMT's pulse–transient characteristic $H(t)$ (Ref. 38):

$$U(t) = \int_0^\infty \bar{U}(\tau)\, H(t-\tau)\, \mathrm{d}\tau\,,$$

where τ is a variable of integration over time. It is related with a spatial variable z for lidar signals as $\tau = 2(R - R_0)/c$. The pulse–transient characteristic can be measured from a PMT's response at its illumination by a short pulse of nanosecond duration. In Ref. 38 the copper–vapor laser radiation of 10 ns duration was used as such a pulse. The photoelectrons of a PMT FEU–104 were recorded with a photon counter having the count rate of 100 MHz and time gate duration of 100 ns.

The function $H(t)$ measured in Ref. 38 and normalized to the value of signal recorded in the first strobe is presented in Fig. 2. As seen from the figure, the peak amplitude of false signals is three orders of magnitude smaller than the level of illuminating signal and slightly decreases with time. As a rule, PMT afterpulsing decreases by an order of magnitude during 100 μs. A slight drop of a PMT's afterpulsing imposes a restriction on the repetition rate of sounding pulses. As was shown in Ref. 39, in ground based sounding the influence of PMT's afterpulsing on lidar signal distortions for altitudes above 12 km becomes considerable for laser pulse repetition rate more than 3 kHz.

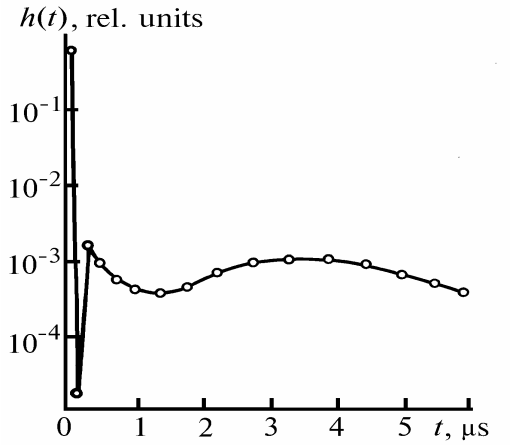

FIG. 2. Pulse-transient characteristic of counting PMT.

To weaken the effect of various nonlinear distortions of lidar signals, modern schemes of lidar recording systems include several PMTs recording portions of a lidar signal in a limited dynamic range from different segments of the sounding paths. The net lidar signal is obtained by joining at the stage of processing.

Output signals of lidar systems should be corrected when appearance of nonlinear distortions of lidar signals fails to be prevented. The simplest correction method is to control carefully the values of the PMT's amplification factor, for example, with the use of a source of reference light pulses[40] and subsequent correction for distortions at signal processing. Since signals of the most of lidar systems are short and include informative fast oscillating components, this way of correction is rarely used. The method of prior determination of a recorder transfer function using simulated optical signals and further correction of recorded signals with a computer is more promising from a practical standpoint. In this case signals are corrected according to the formula[38]

$$\tilde{U}(r) = \frac{U(r) - \sum_{m-1}^{r-1} H(r-m)\, U(m)}{H(0)}\,, \qquad (15)$$

where $U(r)$ is the signal recorded in rth strobe, and $\tilde{U}(r)$ is the corrected signal in the rth strobe.

The third distorting factor is due to the PMT's time lag. In this case the distortion has a form of a decrease in signals due to "sticking" of single–electron pulses. The algorithm for signal correction in this case is considered in Ref. 41. The factor of "sticking" is taken into account by the formula of asymptotically unbiased estimation of the average number of photons $\bar{U}$ detected,

$$\bar{U} = \tilde{U} \exp(-\tilde{U}x)\,; \qquad \bar{U} = U/n, \qquad (16)$$

where $x = \tau_{on}/\tau_d$; τ_{on} is the width of a single–electron pulse at the level of discrimination threshold; τ_d is the strobe duration; n is the number of laser pulses; $\tilde{U}$ is the average number of pulses coming to a PMT; and, $\bar{U}$ is the number of detected single–electron pulses. To solve this nonlinear equation, the following iteration scheme can be used:

$$\tilde{U}^{\,i+1} = \frac{\tilde{U} \exp(x\,\tilde{U}^{\,i}) - x\,(\tilde{U}^{\,i})^2}{1 - x\,\tilde{U}^{\,i}}\,. \qquad (17)$$

5. METHODS FOR NARROWING THE DYNAMIC RANGE OF LIDAR SIGNALS

In a number of practical cases the interval of variation of maximum intensity and the dynamic difference in lidar echo–signal value in a pulse amount to 10^5–10^{12} times over time interval of 10^{-5} s (Ref. 42). To make the dynamic range of lidar echo–signal recorded narrower, four methods are used[43]:

– multiplication of recorded signal by square of time (distance);
– logarithmic amplification of a recorded signal;
– step–by–step transformation;
– strobing.

All these methods are presented and classified in Table I.

The methods of logarithmic transformation and multiplication of recorded signal are the functional ones.

Moreover, the method of multiplication by square distance is nonlinear in time and linear in the amplitude of a recorded lidar return, whereas the method of logarithmic transformation is nonlinear in the amplitude of transformation. Implementation of these methods for narrowing the lidar signal dynamic range is done using optical, photoelectrical, and electronic approaches.

Optical approaches are performed using special vignetting diaphragms, matched filters, and formation of lidar geometrical factor.[44,45]

The use of vignetting diaphragms can result in distortions of lidar returns due to atmospheric turbulence. Matched filters usually reduce the energy potential of a lidar and, correspondingly, the sounding range. Constructions with the use of lidar geometrical factor complicate the lidars, and the required effect in this case is not always attained.

Electronic approaches are normally performed using special amplifying schemes, in particular, logarithmic amplifiers and high–speed electronic switches.[42,46] Among the drawbacks of these approaches there are the following: lidar photoreceivers remain unprotected against the action of strong saturating signals.

Nowadays photoelectronic methods have gained a wide acceptance for narrowing the dynamic range of controlled lidar echo–signals. The input dynamic range of a PMT in logarithmic mode of operation reaches 10^7 with the output dynamic range no more than 1.5 orders of magnitude.[47] However, the logarithmic transformation in PMT, which is based on the effects in dynode system occurring with appearance of a spatial charge between the last dynode and collector, depends not only on the intensity of input signal but also on its shape. This produces significant errors arising in a photodetector at a complicated shape of a lidar return.

By picking the output signal at different dynodes, the dynamic range of lidar signals can be narrowed by five orders of magnitude.[48] However, such a scheme is inapplicable to processing of rapidly varying signals. It does not allow the overloads by strong signal at last dynodes to be taken into account. Negative effects arising here, such as weariness of dynodes, appearance of spatial charges, redistribution of dynodes' potential, take more than 10^{-3} s (Ref. 49) to restore the state of maximum amplification.

PMTs with temporal amplitude adjustment of amplification provide minimum information losses in narrowing the dynamic range of a recorded signal. The adjustment of PMT amplification can be done via power supply voltage,[50] electrical field at modulating electrodes[51] or anodes and dynodes,[52] and external electromagnetic field.[53] Analysis of existing schemes for temporal amplitude adjustment of amplification can be found in Ref. 54.

TABLE I.

Type of adjustment	Methods for narrowing the dynamic range		
	Active		Passive
	Photoelectric	Electronic	Opto-mechanic
Functional	PMT with temporal adjustment according to t^2 law	Amplifier with temporal adjustment of amplification following the t^2 law	Compensating field diaphragms
	Logarithmic PMT	Logarithmic amplifier	Compensating films and wedges
	PMT with adaptive temporal adjustment	Amplifier with an adaptive adjustment of the amplification	
Step-by-step	PMT with step-by-step adjustment	Amplifier with step-by-step adjustment of amplification	Multibase receiving system
	Picking of a signal off the dynode load resistors of a PMT via switching	Amplifier with switching	Several sounding beams Changeable neutral filters Changeable field stops
Strobing	Gating of a photodetector	Strobing amplifier	Mechanic gating Electrooptical gating

TABLE II. Ground–based lidars for sounding H_2O.

Current number	Measurement features				Transmitter				Number of pulses, time of accumulation	Reception scheme	Receiver				Year	Country	References	Notes
	Altitude range, km	Resolution, km	Sensitivity, error	Operating period (d – day, n – night)	Type of laser	Operating wavelength, nm (*), frequency, cm^{-1}	PRF, Hz	Energy per pulse, MJ			Type of telescope	Telescope diameter, cm	Field of view, mrad	Filter width, nm				
1	1.2	0.18			5A	970–976	0.2	1000		3		30	18		1976	United Kingdom	73	Horizontal path
2	< 3	0.3			7B	694.3* 724.348* 724.372*	1	250		1		0.18 m^2	4	20	1979	USA	74	
3	0–3	0.05–1.5		d/n	7A	~ 694*	0.2	1000		1	1	0.15 m^2			1980	Russia	3	
4	1	0.25			6A	5789.61 5788.5	20	60		3A		45	0.56		1982	USA	75	
5	0–7	0.03–0.3	10–15%		1B	724.3 * 723.2*	10	70	$3 \cdot 10^4$			60			1982	France	76	
6	3	0.015	15%			~ 724*						38			1982	France	77	
7	3				1B	~ 720*	10	80				36		2.4	1983	France	78	
8	9	0.1–0.3			1B	~ 724*	10	70		1		60	3	24	1983	France	79	
9	1.5	0.1			5A	10R(18) 10R(20)	0.07	4000		3		30	1		1983	France	80	
10	0–11	0.06–0.3	1–100%	d/n	7A	694.383* 694.3*	0.125	1000	50	1		50	2	1	1984	Russia	81	
11	15	2	50%	d/n	1F	~ 590*	2000	0.5	$8 \cdot 10^5$	1		100			1986	Russia	153	
12	7	0.075	0.7%		5A	10303.5* 10260.4* 10494.5*	30	10–60	$5 \cdot 10^3$						1988	USA	82	Heterodyne reception
13	16	0.2			8	~ 730*	10	50–100				30			1989	France	95	*P* and *T* being measured
14	20	2–3			5A			1–3.5				20			1989	India	95	Heterodyne reception
15	2				5A	10247* 10260*		1000		3A					1990	Italy	83	Horizontal path
16							12	35			1 2	50 28		0.6 8	1990	Germany	84	
17					9	~ 2089	2	10		3A		30			1990	USA	85	
18		0.075–1			1E	~ 720*	20	30				30 50	1.5	0.6	1993	Germany	86	Mobile

TABLE III. Ground–based lidars for sounding the ozone vertical distribution (lidars for sounding the troposphere and the low stratosphere).

Current number	Measurement features				Transmitter				Number of pulses, time of accumulation	Reception scheme	Receiver				Year	Country	References	Notes
	Altitude range, km	Resolution, km	Sensitivity, error	Operating period (d – day, n – night)	Type of laser	Operating wavelength, nm (*), frequency, cm^{-1}	PRF, Hz	Energy per pulse, MJ			Type of telescope	Telescope diameter, cm	Field of view, mrad	Filter width, nm				
1	0.5–2	0.3			5A	9P(14) 9P(24)	1	5500		1		30	4.5		1979	Japan	55	
2	2–12	0.15	10–20%		2B,3A	209.4* 308*	2.5	2–4	4000 8000	1		50	4.8	2.9	1983	Japan	56	
3	0–2.5	0.5		d	2C	277* 317*	80	30		1		25	3	20	1983	Japan	57	
4	Troposphere				9B	288.9* 294.2*		> 50		1	1	40			1990	USA Israel	58	
5	0–3				2C	248–313*	80	~ 300				13			1990	Germany	59	
6	0–15	0.15–1		d/n	9B	266–313*	80	60–250			3	60	2	3.2-6.5	1989	Netherlands	60	
7	0.2–3	0.003–0.6		d/n	2E	248–313*	10	30				40	0.8	4	1993	Germany	61	Mobile
8	0.2–12	0.05–1		d/n	2E	248–313*	80	60–250			2	50	1–10	12	1981	France	159	
9	4–16	0.2–1		d/n	13	280* 295*	20	50			1	61	1.8		1991	USA	62	
10	0–4	0.1		d/n	9B	266* 289*	10	4–50			4	20	1		1990	USA	63	
11	0–12	0.3	10–20%	d/n	14	271* 289*	7000	0.5	15 min	3A		30	2	1.5	1994	Russia	158	Stationary

TABLE IV. Ground–based lidars for sounding the ozone vertical distribution (lidars for sounding the stratosphere).

Current number	Measurement features				Transmitter				Number of pulses, time of accumulation	Reception scheme	Receiver				Year	Country	References	Notes
	Altitude range, km	Resolution, km	Sensitivity, error	Operating period (d – day, n – night)	Type of laser	Operating wavelength, nm (*), frequency, cm^{-1}	PRF, Hz	Energy per pulse			Type of telescope	Telescope diameter, cm	Field of view, mrad	Filter width, nm				
1	2	3	4	5	6	7	8	9	10	11	12	13	14	15	16	17	18	19
1	< 25	0.5	5–20%		3A	307.9* 308.2*	1/15	50	15–45 min	1		50	10	20	1979	Japan	64	
2	10–30	0.75	20–50%		3A	307.9* 308.2*	2	50		1		50	5	20	1980	Japan	65	
3	5–30	0.45 –1.2	5–20%		1H	285–310*	10	40	$3 \cdot 10^4$	1		36	1	3, 70	1982	France	66	
4	20–50	0.1	5–10 μg/m^3		2C		50					60			1983	Germany	68	Container at a helicopter
5	10–25	0.1–1			1H	290–315*	0.1	20–50				0.19 m^2	3–7		1983	Russia	69, 70, 71	
6	< 25	5–20%				296–301*	10	40	15–45 min	1		80	1	70	1983	France	72	
7	5–50		1%		3B	308 * 353*	100	150	$1.5 \cdot 10^6$			60			1984	Germany	89	Container at a helicopter
8	0–40	0.45–1			1H	280–310*	10	20				80	2	3, 70	1985	France	90	
9	2–50	1–3	5%		1H 3G	280–355*	10, 20	40–250	$3 \cdot 10^5$			80			1985	France	67	
10	3–25	1–1.5			2C	290–313*		20–200	$1 \cdot 10^4$						1985	Japan	91	
11	15–50	1–7			3G	308–355*	80, 20	130				80			1986	Japan	92	
12	0–30	1	3–5 * 10^{-11} cm^{-3}		2B	277–360	80	> 30	$1 \cdot 10^4$			50			1987	Japan	93	
13	0–20	1–2				289.294	150	650	$1.5 \cdot 10^5$			90			1987	USA	94	
	15–50	1–5				308.353*	20	50	$1 \cdot 10^7$			40						
14	0–30	0.15–0.8	5%	d	2E	277–360*	80	30	30 min			50	2	2	1987	Japan	95	
15	1.5–50	0.15			3B, 2C	277–351*	250	75–400				200			1989	Japan	95	
16	5–70	0.5–3			3I	289–532*	10–60	15–150				80			1989	Italy	95	
17	40	2–3			5A		cw	1–3.5 W				20			1989	India	95	Heterodyne detector
18	10–25			d	3F	308–532*	1–2	10			2	100		3.6	1990	Russia	96	
19	10–40	1–3			3H	308–532*	20, 80	100, 150				80	1–2	0.9–1.8	1990	Japan	97	
20	12–40	1–3	10–15%		3H	308–532*	20, 80	100, 130	10^3–10^4		1	80	1–2	0.9–1.9	1991	Japan	98	Mobile, temperature

TABLE IV (continued).

1	2	3	4	5	6	7	8	9	10	11	12	13	14	15	16	17	18	19
21	15–45	0.2		n	3C	308–353*	300	100			2	100	0.3–1	3.5	1993	Canada	99	
22	10–40	0.03		d/n	3C	308–353*	300	230			2	100	0.2–1	2	1993	Canada	100	
23	15–50	0.3–5		n	3C	308–355*	200	100–500			3	100	0.4	< 2	1993	USA	101	
24	10–50	0.5–5		n	3C	308–353*	20	300				60	0.4	5	1993	Germany	102	
25	15–50	0.5–8		n	3G	308–355*	50	120, 300			1	80	1.3	20	1993	France	103	
26	3–30	0.015		n		289–294*	10	50			1	40	1–5	< 1	1993	USA	104	
27	5–35	0.03–0.3		d/n	10	300–350*	10	100–1000			1	60	0.15–1.5	0.2	1993	Germany	105	
28	2–40	0.15		d/n	3I	299–355*	10, 80	110–150			1	80	1		1993	Italy	106	Monochromator
29	15–45	0.3–5		n	3E	308–353*	250	400			2	81	0.5	2	1993	Netherlands	107	
30	15–40	1–5		n	3G	308–355*	20, 80	110, 130			1	80	1–2	1–2	1993	Japan	108	
31	10–50	0.1–1		n	3C	308–353*	50–80	20, 40				220	0.3±1	1–2	1993	Russia	154	
32	0–35				2D	339–351*	10					200				Japan	95	
					3D							2						
33	20–45	0.5–2			3G	308–355*	10, 50	100, 200				0.5 m^2			1989	France	95	
34	20–42				3G	308–355*		2, 20 W			3	75			1989	USA	95	
35					3C	308–355*	300	10–125			2	100	0.8	3.5	1989	Canada	95	
36	10–50	0.1	10–20%	n	3C, 3F	308–353*	60	60	15–20 min		2	100	2	3	1992	Russia	157	Stationary

TABLE V. Lidars for pollution monitoring.

Current number	Gas	Measurement features				Transmitter				Number of pulses, time of accumulation	Reception scheme	Receiver				Year	Country	References	Notes
		Altitude range, km	Resolution, km	Sensitivity, error	Operating period (d – day, n – night)	Type of laser	Operating wavelength, nm (*), frequency, cm^{-1}	PRF, Hz	Energy per pulse, MJ			Type of telescope	Telescope diameter, cm	Field of view, mrad	Filter width, nm				
1	2	3	4	5	6	7	8	9	10	11	12	13	14	15	16	17	18	19	20
1	NO_2	1	0.1	0.05		1A	448.8* 448.1 446.5 441.8		4-8	1			20			1974	USA	109	
2	SO_2 O_3	1	0.07	0.06 0.12 ppm*km		1G	292.3* 293.3 294.0	0.017	0.3	8			7			1975	USA	110	

TABLE V (continued).

1	2	3	4	5	6	7	8	9	10	11	12	13	14	15	16	17	18	19	20
3	SO_2 NO_2	5	0.5	20 ppb 10 mg/m^3		1G	298.0* 299.0 458.2 456.8	10–25	0.4 0.5		3A	2	25	2	5–10	1979	Sweden	111	
4	SO_2					1H	300.01* 299.5		0.1		1	2	26	0.017	10	1979	USA	112	
5	CO	2.5				5B	2154–2086	300	1		3	1	30	1.1		1980	USA	113	
6	H_2O CH_4	2		0.25 Torr 10 ppb		5A	10246.6* 10260.4 10532.1 10571.0	70	1.3				60			1980	USA	114	
7	Hg	1		4 ng/m^3		1I	253.65* 253.68	10	0.7			2	25		20	1982	Sweden	160	
8	SO_2 NO_2			30 mg/m^3		1H 1B	299.3 * 300.05 448.1 446.5				3	2	30			1983	Sweden	115	
9	SO_2 O_3	3 2.5	0.4 0.15–0.5	20%		1H	300.01* 299.65 284.5 289.5	10	12 10	2000 10^4			60 36			1984	France	116	
10	H_2O O_3	9 30	0.1–0.3 0.451.2			1B 1H	724–855* 310	10	70–40	50 min			60 36	3 1	24 3–70	1983	France	79	
11	HCl	2	0.1	300 ppb		13	3636.3 3698.3	1	10	100			50			1984	Germany	117	Istalled onboard a ship
12	O_2	1.6	0.008	0.3%		1H	760.2* 759.3	10	100	100			45			1989	USA	118	
13	NO_2	3	0.05–0.2			1C	447.9* 446.5	10	20				50			1986	Japan	92	Pressure being measured
14	H_2O	0.5	0.0075			6B	9347* 10600						30			1987	Russia	155	
15	H_2O CH_4 HCl	3	0.2			12	~ 1751.5 ~ 1750. ~ 1750.	3	10	25			30			1987	USA	119	

TABLE V (continued).

1	2	3	4	5	6	7	8	9	10	11	12	13	14	15	16	17	18	19	20
16	NO NO_2					1K 1E	226.8* 224.5 448.1 453.6	80	5 3			2	40			1989	Germany	133	
17	NO_2	6	0.1–1		d/n	1H	~ 450	10	5			1	28	2	10	1993	Netherlands	120	
18	H_2O O_3	3 5	0.015		d/n	5A	9200–10800*	1	4000			2	38	1		1993	Italy		
19	H_2O O_3	10 30	0.015		n	8 2A	700–800* 248	20	200			5	50	1–4	2	1993	Japan	121	
20	H_2O CO_2	1–6	0.3			9 9A	~2000 ~1000	5	150			2	40	1–4		1993	USA	122	
21	NO NO_2 SO_2 O_3	10	0.0015–0.2		d/n	1K	220–350*	80	2–5			1	60	0.15–1.5	0.5–1	1993	Germany	123	
22	NO NO_2 N_2O SO_2 CH_4 C_6H_6	10	0.2–0.5		d/n	10B	220–2200*	10	100–1000			1	30	0.5–2	0.5	1984	France	151	

TABLE VI. Airborne lidars for different purposes.

Current number	Gas	Measurement features				Transmitter				Number of pulses, time of accumulation	Reception scheme	Receiver				Year	Country	References	Notes
		Altitude range, km	Resolution, km	Sensitivity, error	Operating period (d – day, n – night)	Type of laser	Operating wavelength, nm (*), frequency, cm^{-1}	PRF, Hz	Energy per pulse			Type of telescope	Telescope diameter, cm	Field of view, mrad	Filter width, nm				
1	2	3	4	5	6	7	8	9	10	11	12	13	14	15	16	17	18	19	20
1	O_3	Downward from 23 and 36 2.5	0.15	20–50%		1L	282* 355*	10	1–3			1	30			1983	USA	138	Balloonborne
2	O_3	down to 3.2	0.21	5 ppb 10%		1H	285.9* 299.4*	1–10	30	100		1	35	< 2	0.3	1993	USA	139	

TABLE VI (contibued).

1	2	3	4	5	6	7	8	9	10	11	12	13	14	15	16	17	18	19	20
3	O_3	down to 1.7	0.15	20 ppb 20–40%	d	5A	9P(14), 9P(24)	0.25	300	200		2	30			1989	Japan	140	
4	O_3	1–6 18–26	0.35 0.5	10– 40 ppb	n	1H	286–311*	10			3		40			1991	USA	141	
5	O_3	1–3 down-ward	0.007 –0.1		d/n	2E	248–313*	30–50	300				35	1	20	1991	USA	142	
6	O_3	0–15	0.15		d/n	9B	266–290*	10	30			1	40	1–6	2	1989	Canada	134	
7	O_3	1–10 down-ward upward	0.2		d/n	1H	286–300*	10	30				35	< 1.25		1989	USA	144	
8	O_3	5	0.21	5 ppb		1H	~ 300*	10	40–80				35			1982	USA	145	
	H_2O	1.5		10^{-3}		1B	~ 700*	10	50										
9	O_3	3.6	0.3		d/n	2E	277–360*	20	30–60				50	0.5–1	7–15	1991	USA	146	
	SO_2																		
10	H_2O	4	0.05	0.002		1B	723.2*	10	50	200			35			1982	USA	147	
11	SF_6					5A	10.510 9.460	cw	3 W		2		7.5			1978	Germany	148	
12	H_2O	7	0.1–0.2		d/n	1B	~ 724*	1–10	30–40			1	35	1.3	0.6	1989	Germany	149	
13	O_3	3	0.1			2E	277–360*	20	30–60				50			1989	USA	95	
	SO_2																		
	NO_2																		
14	O_3	1.6	20 ppb			1H	292–298*	5	10				45			1984	USA	150	Pressure and
	H_2O		10%			1B	~ 724*		60										temterature
			10%			8	~ 940*		50–100										being measured
15	H_2O	0.2–10			d/n	8	726.5* 732*		150		1	3	38			1990	USA	33	
16	H_2O	1–7 down-ward	0.2			8	~ 727*	10	30–100				35	< 1.25	0.5	1990	USA	152	
17	H_2O	0.8–2	0.15			1B	~ 720*	10	30				40			1983	Germany	161	

TABLE VII. Mobile lidars for pollution monitoring.

Current number	Gas	Measurement features				Transmitter				Number of pulses, time of accumulation	Reception scheme	Receiver				Year	Country	References	Notes
		Altitude range, km	Resolution, km	Sensitivity, error	Operating period (d – day, n – night)	Type of laser	Operating wavelength, nm (*), frequency, cm^{-1}	PRF, Hz	Energy per pulse, MJ			Type of telescope	Telescope diameter, cm	Field of view, mrad	Filter width, nm				
1	2	3	4	5	6	7	8	9	10	11	12	13	14	15	16	17	18	19	20
1	SO_2	3	0.1	30 ppb			299.22* 300.0						50			1981	USA	124	
2	SO_2	3	0.015–0.2	25 ppb		1H	300.05* 299.38	10	10	1–1000			50			1982	USA	125	
3	SO_2	2.5	0.01	1 ppm		1H	300.2* 299.5	10	10	1000			45			1983	Russia	126	
4	SO_2	3	0.015–0.2	50 ppb		1H	~ 300*	10	30	300			56			1984	Italy	127	
5	SO_2 NO_2	3	0.3	15 ppb 10 ppb		1G 1A	296.17* 297.35 448.1 449.8	0.5	10–60 100–300	120			60			1984	Germany	128	
6	H_2O	6	0.1–0.3	3–10%		5A	10246.6* 10260.4 10303.5 9305.4 9282.4	15–20	40–50	600			22			1987	USA	129	Heterodyne detector
7	SO_2 NO_2	1.5 3	0.1 0.03	15 25 μg/m^3		1H 1C	300.05* 299.3 448.1 446.5	10 10	2	1000			30			1987	Russia	155	
8	SO_2 NO_2	3 6	0.015 0.015	25 15 μg/m^3		1H	300.03* 299.33 ~ 450	5	5	400	3A		40	2		1987	Sweden	130	
9	NO_2	3	0.1–0.3	3 ppb		1C	448.1* 446.6	10	20	6000			50			1987	Japan	156	
10	Cl_2	1	0.25	170 μg/m^3		1H	308* 298	10	2	140			30			1987	Sweden	131	

TABLE VII (continued).

1	2	3	4	5	6	7	8	9	10	11	12	13	14	15	16	17	18	19	20
11	NO	1	0.35	3 μg/m^3		9C	226.812* 226.824	5	3–5				40			1989	Germany	132	
12	NO_2 NO	1		1 0.1 ppm*m		1E 1K	448.1* 453.6 226.8 224.05	80	30 5			2	40			1989	Germany	133	
13	Hg	1		2 ng/m3		1K	253.652* 253.66	5	5			2	40			1989	Sweden	134	
14	NO_2	2	0.1			1H	448.1* 449.9	10	5	1000 4000						1990	Netherlands	135	
15	NO NO_2 SO_2 O_3	10	0.01–1		d/n	1E, 1K	225–440*	100	4–50			1	60	3	0.2–5	1993	Switzerland	136	
16	NO NO_2 O_3 SO_2 C_2H_4 C_6H_6	3	0.012			1H 9A	UV–IR	10	0.01–1			3	50	1		1993	United Kingdom	137	

6. LIDARS FOR SOUNDING THE ATMOSPHERIC AND POLLUTING GASES

In this section we present information about differential absorption lidars constructed in last 15 years by different groups. This information is tabulated in Tables II–VII. Tables II–V present the lidars for sounding humidity, ozone, and polluting gases, respectively. Table VI gives information about airborne lidars, whereas Table VII is devoted to description of mobile lidars.

The tables have the following blocks: a) measurement features, b) transmitter, and c) receiver. Each block contains a detailed information. Presented in column 6 is the number of a laser type, whereas the data on lasers used are presented in Table VIII. Columns 11 and 12 give the numbers of lidar optical scheme (see Fig. 3) and type of the telescope. Telescopes are listed in the following order: Cassegrenian telescope (*1*), Newton one (*2*), Dal'–Kirkham one (*3*), Newton telescope with parabolic mirror (*4*), and Konde–Newton one (*5*). Presented in the last columns of Tables II–VII are the year of publication, the country, and the number of reference.

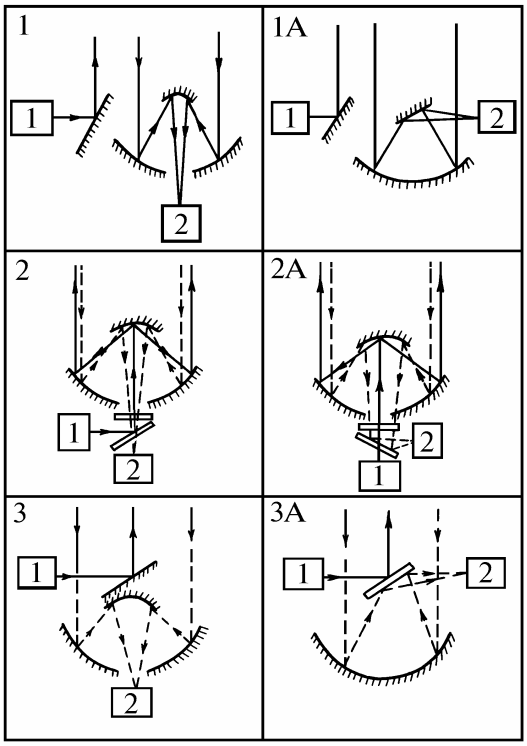

FIG. 3. Versions of optical "transmitter-receiver" schemes used in lidars: transmitter (1) and receiver (2).

TABLE VIII. Types of laser sources.

1. Dye laser

1A. dye laser with flash-lamp pumping,

1B. dye laser pumped by second harmonic of Nd:YAG laser,

1C. dye laser pumped by third harmonic of Nd:YAG laser,

1D. dye laser pumped by nitrogen laser,

1E. dye laser pumped by XeCl laser,

1F. dye laser pumped by copper vapor laser,

1G. second harmonic of dye laser with flash-lamp pumping,

1H. second harmonic of dye laser pumped by second harmonic of a Nd:YAG laser,

1I. second harmonic of dye laser pumped by third harmonic of a Nd:YAG laser,

1J. second harmonic of dye laser pumped by nitrogen laser,

1K. second harmonic of dye laser pumped by XeCl laser,

1L. anti–Stokes in H_2 from second harmonic of dye laser pumped by second harmonic of a Nd:YAG laser.

2. KrF laser

2A. KrF laser,

2B. KrF laser with CH_4 SRS cell,

2C. KrF laser with H_2 and CH_4 SRS cell,

2D. KrF laser with H_2 and D_2 SRS cell,

2E. KrF laser with H_2, D_2, and CH_4 SRS cell.

3. XeCl laser

3A. XeCl laser,

3B. XeCl laser with CH_4 SRS cell,

3C. XeCl laser with H_2 SRS cell,

3D. XeCl laser with D_2 SRS cell,

3E. XeCl laser with H_2 and D_2 SRS cell,

3F. XeCl laser with second harmonic of Nd:YAG,

3G. XeCl laser with third harmonic of Nd:YAG,

3H. XeCl laser with second and third harmonics of Nd:YAG,

3I. XeCl laser with SRS cell with second harmonic of Nd:YAG,

4. XeF laser

5. CO_2–laser

5A. pulse TEA CO_2–aser,

5B. second harmonic of CO_2–laser.

6. Parametric light generator (PLG)

6A. PLG pumped by first harmonic of Nd:YAG,

6B. PLG pumped by second harmonic of Nd:YAG,

7. Ruby laser

7A. ruby laser,

7B. ruby laser with dye laser pumped by ruby laser.

8. Alexandrite laser

9. Nd:YAG laser

9A. Nd:YAG laser,

9B. fourth harmonic of Nd:YAG laser with H_2 and D_2 SRS cell,

9C. Nd:YAG laser radiation mixed with second harmonic of dye laser pumped by second harmonic of Nd:YAG.

10. Titanium sapphire laser

10A. titanium sapphire laser and its second and third harmonics,

10B. titanium sapphire laser radiation mixed with its second and third harmonics.

11. Ho:YSGG laser and Nd:YAG

12. Co:MgF2 laser pumped by Nd:YAG radiation

13. DF laser

14. Cu laser

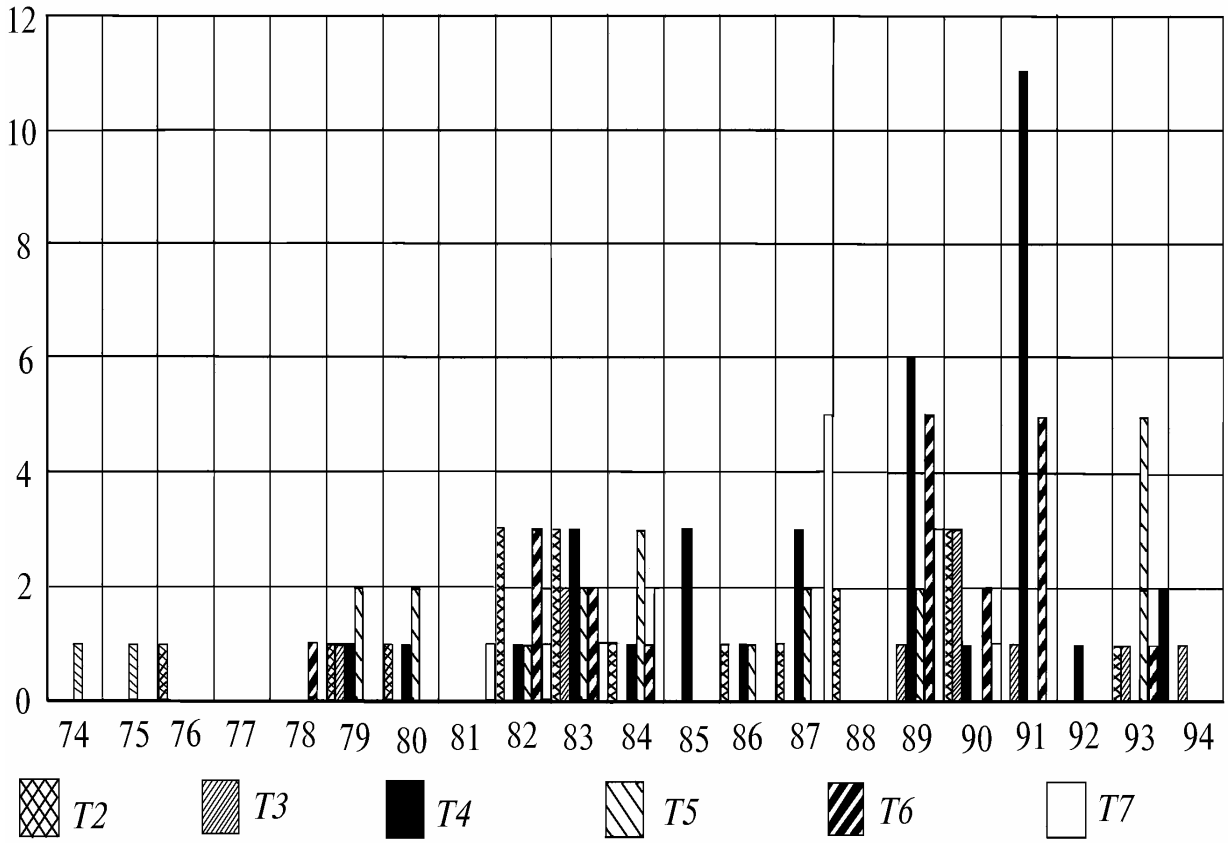

FIG. 4. Histograms of papers published in years. Marks T2–T7 correspond to the numbers of tables.

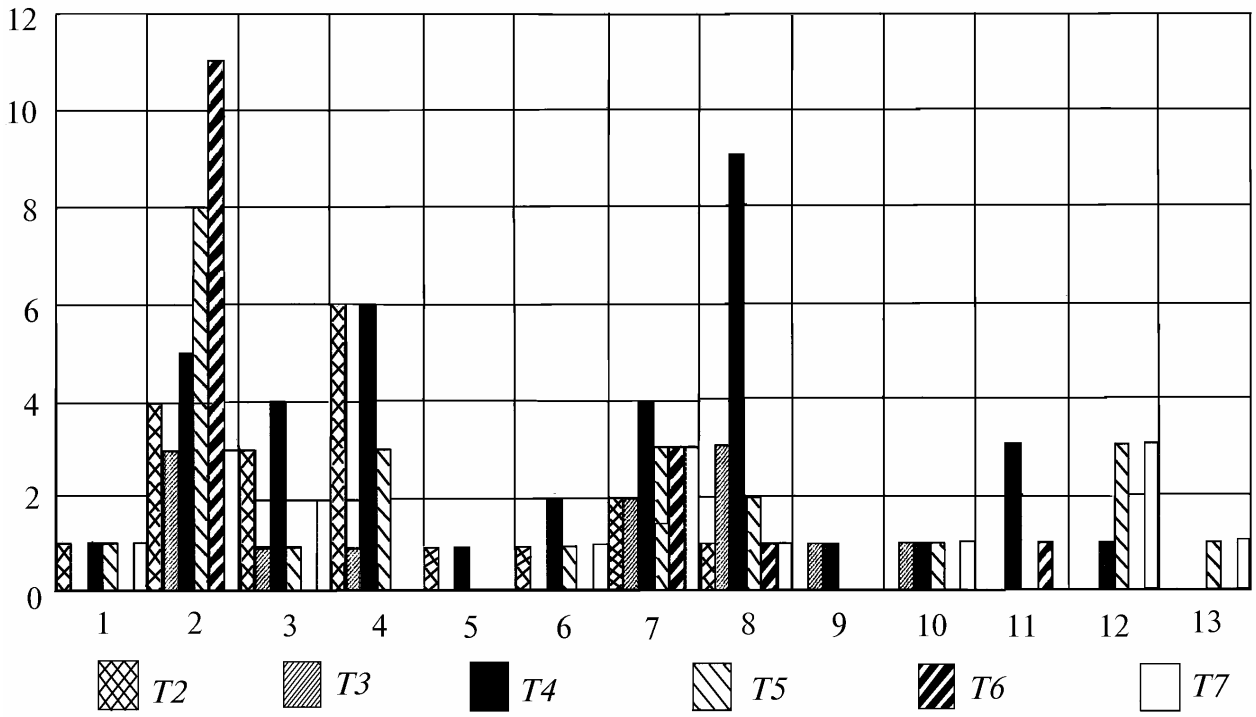

FIG. 5. Histograms of papers published in countries: United Kingdom (1), USA (2), Russia (3), France (4), India (5), Italy (6), Germany (7), Japan (8), Israel (9), Netherlands (10), Canada (11), Sweden (12), Switzerland (13). Marks T2–T7 correspond to the numbers of tables.

Time histograms of publications for years and countries are shown in Figs. 4 and 5. One can see that in the field of H_2O sounding the USA, France, Germany, and Russia are leading countries, as to ozone sounding the leaders are Japan, USA, Germany, and Russia, and in the field of sounding of polluting gases the leaders are Sweden, Germany, USA, and Japan. The USA is certainly the leader in airborne lidars.

REFERENCES

1. V.M. Zakharov and O.K. Kostko, *Lasers and Meteorology* (Gidrometeoizdat, Leningrad, 1972), 175 pp.
2. V.E. Zuev, *Laser–Meteorogist* (Gidrometeoizdat, Leningrad, 1974), 96 pp.
3. V.M. Zakharov and O.K. Kostko, *Meteorological Lidar* (Gidrometeoizdat, Leningrad, 1977), 203 pp.
4. E.D. Hinkly, ed., *Laser Monitoring of the Atmosphere* (Springer Verlag, New York, 1976).
5. V.M. Zakharov, ed., *Lasers as Applied to Determination of Composition of the Atmosphere* (Gidrometeoizdat, Leningrad, 1983), 218 pp.
6. R.M. Measures, *Laser Remote Sensing* (Willey, New York, 1987).
7. V.E. Zuev and V.V. Zuev, *Remote Optical Sounding of the Atmosphere* (Gidrometeoizdat, St. Petersburg, 1992), 232 pp.
8. G. Fiocco and L.D. Smullin, Nature **199** (1963).
9. V.E. Zuev and I.E. Naats, *Inverse Problems of Laser Sounding of the Atmosphere* (Nauka, Novosibirsk, 1982), 241 pp.
10. R.M. Schotland, in: *Proc. of Third Symp. on Remote Sensing of Environment*, Univ. Michig. Ann. Arbor., Mishigan (1964), pp. 215–224.
11. M.L. Wright, E.K. Prootor, L.S. Gasiorek, et al., Final Report SKI Project 1966. Contract NASA–11657, Hampton, Virginia: NASA Langley Research center (1975).
12. R.M. Measures and G.A. Pilon, Opto–Electron. **4**, 141–153 (1972).
13. R.L. Byer and M. Gurbuny, Appl. Opt. **12**, No. 8, 1496–1505 (1973).
14. R.M. Schotland, J. Appl. Meteorol. **13**, 71–77 (1974).
15. V.E. Zuev, Yu.S. Makushkin, V.N. Marichev, et al., Appl. Opt. **22**, No. 23., 3733–3741 (1983).
16. O.K. Voitsekhovskaya, Yu.S. Makuskin, A.A. Mitsel', et al., Izv. Vyssh. Uchebn. Zaved. SSSR, ser. Fiz. **1**, 62–70 (1977).
17. V.N. Marichev and A.A. Mitsel', Izv. Vyssh. Uchebn. Zaved. SSSR, ser. Fiz. **3**, 47–51 (1985).
18. V.N. Marichev, A.A. Mitsel', and I.I. Ippolitov, in: *Spectroscopic Methods of Sounding of the Atmosphere* (Nauka, Novosibirsk, 1985), pp. 4–57.
19. S. Ismail and E.V. Browell, Appl. Opt. **28**, No. 17, 3603–3615 (1989).
20. A.A. Mitsel', *"Numerical simulation of problems of laser sounding of the atmosphere using differential absorption method,"* Author's Abstract of the Cand. Phys.–Math. Sci. Dissert., Tomsk (1982).
21. V.V. Zuev, A.A. Mitsel', and I.V. Ptashnik, Atmos. Oceanic Opt. **5**, No. 10, 672–673 (1992).
22. Yu.E. Voskoboinikov and A.A. Mitsel', Izv. Akad. Nauk SSSR, ser. Fiz. Atmos. Okeana **17**, No. 2, 175–181 (1981).
23. Yu.E. Voskoboinikov, M.Yu Kataev, and A.A. Mitsel', Atm. Opt. **4**, No. 2, 177–184 (1991).
24. O.K. Kostko, Kvant. Elektron. **2**, No. 10, 2133–2166 (1975).
25. H. Kildal and R.L. Byer, Proc. IEEE. **59**, No. 12, 5–30 (1971).
26. R.L. Byer, Opt. Quant. Electron., No. 7, 147–177 (1975).
27. V.E. Derr and C.G. Little, Apl. Opt. **9**, No. 9, 1976–1992 (1970).
28. W.B. Grant, Optical Engin. **30**, No. 1, 40–48 (1991).
29. V.V. Zuev, Yu.N. Ponomarev, A.M. Solodov, et al., Opt. Lett. **10**, No. 7, 318–320 (1985).
30. C.L. Korb and C.Y. Weng, in: *Proc. Eleventh ILRC*, Madison. Wisc. American Meteorological Society (1982), Vol. 78.
31. S. Ismail, E.V. Browell, G. Megie, et al., in: *Conference Digest. Twelfth ILRC*, Aixen–Provence, France (1984), p. 431.
32. A. Ansmann, Appl. Opt. **24**, No. 21, 3476–3480 (1985).
33. S. Ismail and E.V.Browell, in: *Abstracts of Reports at the Thirteenth ILRC*, Toronto, Canada (1986).
34. L. Lading, A.S. Jensen, E. Rasmussen, et al., in: *Proc. Conf. Groun Based Remote Sensing Techniques for the Troposphere,* Hamburg (1986), pp. 31–44.
35. J. Bosenberg, A. Ansmann, and H. Linne, *ibid.*, pp. 81–90.
36. F.A. Theopold and J. Bosenberg, in: *Proc. Fifteenth ILRC*, Tomsk, Russia (1990), pp. 173–176.
37. A.I. Nadeev and K.D. Shchelevoi, in: *Abstracts of Reports at 8th All–Union Symposium on Laser and Acoustic Sensing of the Atmosphere*, Tomsk (1984), Vol. 2, pp. 310–313.
38. Yu.F. Arshinov, S.M. Bobrovnikov, V.E. Zuev, et al., in: *Proc. Twelfth ILRC*, Aix-en–Provance, France (1984), pp. 135–137.
39. A.V. El'nikov, V.N. Marichev, S.I. Tsaregorodtsev, et al., in: *Proc. 10th All–Union Symposium on Laser and Acoustic Sensing of the Atmosphere,* Tomsk (1989), Vol. 2, pp. 266–270.
40. Yu.M. Andreev, R.I. Gavrilovskii, and V.V. Zuev, Inventor's Certificate No. 1595182, May 22, 1990.
41. V.G. Astafurov and A.A. Mitsel', Avtometriya, No. 1, 92–97 (1984).
42. O.E. Yakimovich, in: *Abstracts of Reports at 13th All–Union Scientific–Technical Conference on High–Speed Photography, Photonics, and Metrology of Fast Processes,* Moscow (1987), p. 86.
43. A.A. Tikhomirov, in: *Proc. 7th All–Union Symposium on Laser and Acoustic Sounding of the Atmosphere*, Tomsk (1982), pp. 173–176.
44. B.I. Metlitskii and E.A. Chayanova, in: *Reports of Central Aerological Observatory* (Gidrometeoizdat, Moscow, 1977), pp. 81–89.
45. A.A. Tikhomirov, in: *Proc. 6th All–Union Symposium on Laser and Acoustic Sounding of the Atmosphere*, Tomsk (1980), pp. 53–57.
46. V.M. Volkov, A.V. Dmitriev, and A.A. Ivan'ko, *Functional Amplifiers with Wide Dynamic Range* (Sov. Radio, Moscow, 1976), 157 pp.
47. V.V. Bacherikov, V.E. Kachain, and Yu.A. Makarov, Prib. Tekh. Eksp., No. 6, 166–168 (1974).
48. V.I. Il'in, G.I. Il'in, and Yu.E. Pol'skii, in: *Proc. 5th All–Union Symposium on Laser and Acoustic Sounding of the Atmosphere*, Tomsk (1978), pp. 92–95.
49. A.G. Berkovskii, V.A. Gavanin, and I.N. Zaidel', in: *Vacuum Photoreceiving Devices* (Energia, Moscow, 1976), 187 pp.
50. L.M. Kleinerman, N.V. Kigel', and N.S. Gibaidulin, Opt. Mekh. Promst., No. 1, 63–64 (1971).
51. L. Barisas and M. Leiter, PNI, No. 1, 81 (1980).
52. Yu.V. Popov and B.I. Uzhenkov, Opt. Mekh. Promst., No. 2, 65–71 (1976).
53. Yu.V. Popov and B.I. Uzhenkov, Prib. Tekh. Eksp., No. 2, 158 (1972).

54. V.I. Ivanov, I.A. Malevich, and A.P. Chaikovskii, *Multi–Purpose Lidar Systems* (State University, Minsk, 1986), 166 pp.
55. K. Asai, T. Itabe, and T. Igarashi, Appl. Rhys. Lett. **35**, No. 1, 60–62 (1979).
56. O. Uchino, M. Tokunaga, M. Maeda, et al., Opt. Lett. **8**, No. 7, 347–349 (1983).
57. M. Maeda, T. Shibata, and U. Kyusshu, in: *Proc. CLEO* (1988), pp. 56–57.
58. D.A. Haner, M. Kleiman, and I.S. McDermid, in: *Proc. Fifteenth ILRC,* Tomsk, Russia (1990), Vol. 1, pp. 195–198.
59. W. Carnuth, U. Kempfer, and R. Lotz, *ibid.*, pp. 202–205.
60. A. Apituley, *Report TESLAS* (1989).
61. Ch. Senff, J. Bosenberg, and G. Peters, J. Atm. Oc. Techn. (1993)
62. M.H. Proffitt and O. Longford, SPIE, No. 1491, 2–6 (1991).
63. Y. Zhao, M.J. Post, and R.M. Hardesty, Appl. Opt. **29**, 4111–4119 (1990).
64. O. Uchino, M. Maeda, and M. Hikono, IEEE Quant. Electr. **QE15**, No. 10, 1094–1107 (1979).
65. O. Uchino, M. Maeda, T. Shibata, et al., Appl. Opt. **19**, No. 24, 4175–4181 (1980).
66. P.H. Flamant, J. Pelon, J. Lefrere, et al., AIAA, No. 88–0010 (1982).
67. G. Megie, J. Pelon, J. Lefrere, et al., in: *Proc. Optical and Laser Remote Sensing*, ed. by D.K. Killinder (1983), pp. 223–228.
68. J. Werner, K.W. Rothe, and H. Wather, Appl. Phys. B. **32**, 113–118 (1983).
69. V.P. Gusarov, A.P. Prokhorov, N.D. Smirnov, et al., in: *Proc. 6th All–Union Symposium on Laser and Acoustic Sounding of the Atmosphere*, Tomsk (1980), Vol. 2, pp. 6–8.
70. V.P. Gusarov, O.K. Kostko, A.P. Prokhorov, and N.D. Smirnov, in: *Proc. 6th All–Union Symposium on Laser and Acoustic Sounding of the Atmosphere*, Tomsk (1980), Vol. 1, pp. 222–224.
71. I.M. Nazarov, A.N. Nikolaev, and Sh.D. Fridman, *Foundations of Remote Methods for Environmental Pollution Monitoring* (Gidrometeoizdat, Leningrad, 1983), 280 pp.
72. J. Pelon and G. Megie, Planet. Sci. **31**, No. 7, 717–721 (1983).
73. E.R. Murray, R.D. Hake, Jr.J. van de Laan, et al., Appl. Phys. Lett. **28**. No. 9, 542–543 (1976).
74. E.V. Browell, T.D. Wilkerson, T.J. McCllrath, Appl. Opt. **18**, No. 20, 3474–3483 (1979).
75. D.J. Brassington, Appl. Opt. **21**, 4411–4416 (1982).
76. C. Cahen, G. Megie, and G. Flamant, Appl. Meteor. **21**, 1506–1515 (1982).
77. C. Cahen, J.L. Lesne, J.M. Michelin, et al., NASA Conf. Publ., No. 2228, 37–40 (1982).
78. R.T. Menzies and G. Megie, in: *Proc. Optical and Laser Remote Sensing*, ed. D.K. Killinger (1983), pp. 170–175.
79. G. Megie, J. Pelon, C.Cahen, et al., in: *Proc. Optical and Laser Remote Sensing*, ed. D.K. Killingere (1983), pp. 123–128.
80. P.W. Baker, Appl. Opt. **22**, No. 15, 2257–2264 (1983).
81. V.V. Zuev and V.E. Zuev, in: *Proc. Twelfth ILRC*, Aix-en–Provance, France (1984), pp. 165–166.
82. W.B. Grant, A.M. Brothers, and J.R. Bogan, Appl. Opt. **22**, 26–90 (1983).
83. V.V. Zuev and O.A. Romanovskii, Zh. Prikl. Spektrosk. **34**, 519–523 (1986).
84. R. Barbini, F. Colao, A. Polucci, et al., in: *Proc. Fifteenth ILRC,* Tomsk, Russia (1990), pp. 156–159.
85. J. Bosenberg, C. Senff, and P.–Y. Thro, in: *Proc. Fifteenth ILRC*, Tomsk, Russia (1990), Vol. 2, pp. 170–172.
86. D.K. Killinger, S.D. Cha, K. Chan, et al., in: *Proc. Fifteenth ILRC*, Tomsk, Russia (1990), Vol. 2, pp. 372–374.
87. F.A. Theopold and J. Bosenberg, J. Atm. Oc. Technol. (1993).
88.T. Itabe, M. Ishizu, T. Aruge, et al., CLEO (1987), pp. 128–129.
89. I.V. Samokhvalov, ed., *Spectroscopic Methods for Sensing the Atmosphere* (Nauka, Novosibirsk, 1985), 144 pp.
90. J. Werner, W. Rothe, and H. Walther, in: *Conf. on Lasers and Electr.* (1984), *Dig. Techn. Pap.,* pp. 74–75.
91. G. Megle, G. Ancellent, and J. Pelon, Appl. Opt. **24**, No. 21, 3454–3463 (1985).
92. T. Sibata, K. Seki, T. Khayama, et al., Fedza Kenko **13**, 276–289 (1985).
93. M.P. McCormic, compiler, *First Intern. Lidar Research Directory*, NASA (1986).
94. T. Shibata, T. Fukuda, T. Narikiyo, et al., Appl. Opt. **26**, No. 13, 2604–2608 (1987).
95. I.S. McDermid, Serv. in Geophys. **9**, 107–122 (1987).
96. M.P. McCormic, compiler, *Second Intern. Lidar Research Directory*, NASA (1989).
97. A.V. El'nikov, V.N. Marichev, and V.V. Zuev, in: *Proc. Fifteenth ILRC*, Tomsk, Russia (1990), Vol. 1, pp. 214–217.
98. O. Uchino, in: *Proc. Fifteenth ILRC*, Tomsk, Russia (1990), Vol. 2, pp. 252–255.
99. O. Uchino and I. Tabata, Appl. Opt. **30**, No. 15, 2005–2012 (1991).
100. A.I. Carswell, S.R. Pal, and W. Steinbrecht, Can. J. Phys. **69**, 1076–1086 (1991).
101. A. Ulitsky, T.Y. Wang, et al., *Proc. Sixteenth ILRC. NASA Conf. Publ.*, No. 3158, pp. 434–449 (1992).
102. D.A. Haner and I.S. McDermid, IEEE Quant. Electr. **QE–26**, 1292–1298 (1990).
103. H. Claude and W. Wandersee, in: *Proc. Fifteenth ILRC*, Tomsk, Russia (1990), Vol. 1, pp. 206–209.
104. S. Godin, G. Megie, and J. Pelon, GRL **16**, No. 6, 162–168 (1989).
105. I.S. McDermid, S.M. Godin, R.A. Barnes, et al., JGR **95**, 10037–10042 (1990).
106. M.H. Beniston–Rebertz, H. Kolsh, P. Rairoux, et al., JGR **95**, D7, 9879–9884 (1990).
107. L. Stefannutti, M. Morandi, and D.Guasta, JGR **96**, No. 12, 975 (1991).
108. D.P. Swart and J. Spakman, in: *RIVM Report*, No. 850024001 (1992).
109. O. Uchino and T. Fujimoto, J. Geomagn. Geoelectr. **44**, 19–25 (1992).
110. A.V. El'nikov, V.V. Zuev, V.N. Marichev, et al., Atmos. Oceanic Opt. **5**, No. 6, 362–369 (1992).
111. W.B. Grant, R.D. Hake, E.M. Liston, et al., Appl. Phys. Lett. **24**, No. 11, 550 (1974).
112. W.B. Grant and R.D. Hake, Appl. Phys. **46**, No. 7, 3019–3023 (1975).
113. K. Fredriksson, B. Galle, K. Nystrom, et al., Appl. Opt. **18**, No. 17, 2998–3003 (1979).
114. R.S. Adrain, D.J. Brassington, S. Sutton, et al., Optical Quant. Electr., No. 11, 253–264 (1979).
115. N. Menyuk, D.K. Killinger, and W.E. DeFeo, Appl. Opt. **21**, No. 12, 2275–2286 (1982).
116. K.W. Rothe, Radio Electr. Engin. **50**, 567–574 (1980).
117. K. Fredriksson and S. Svanberg, in: *Proc. Optical and Remote Sensing*, ed. E.K. Killinger (1983), pp. 148–155.

118. R. Capitini, G. Ancelent, G. Megie, et al., in: *Proc. Twelfth ILRC*, Aix-en–Provance, France (1984), pp. 269–273.
119. H.J. Heinridi, C. Weitkamp, R. Banmgard, et al., in: *Proc. IGARSS* (1984), pp. 679–684.
120. G.K. Schwemmer, C.L. Korb, M. Dombrowski, et al., in: *Proc. IGARSS* (1984), pp. 512–516.
121. A.P. Kubyshkin, V.I. Kuznetsov, A.V. Migulin, et al., Izv. Akad. Nauk SSSR, Fizika **51**, 219–223 (1987).
122. N. Menyuk and D.K. Killinger, Appl. Opt. **26**, No. 15, 3061–3065 (1987).
123. D.P.J. Swart and J. Bergwerf, in: *Proc. Fifteenth ILRC*, Tomsk, Russia (1990), Vol. 2, pp. 80–83.
124. T. Shibata, M. Maeda, et al., J. Geomagn. Geoelectr. **41**, 303–316 (1989).
125. S. Cha, K.P. Chan, and D.K. Killinger, Appl. Opt. **30**, 3938 (1991).
126. H. Kolsh, P. Rairoux, J.P. Wolf, et al., Appl. Opt. **28**, 2052–2056 (1989).
127. J.G. Hawley, Laser Focus., March, 60 (1981).
128. J.G. Hawley, and E.E. Uthe, in: *Proc. Conf. Remote Sensity and the Atmosphere* (1984), pp. 193–201.
129. Yu.G. Vainer, I.P. Malyavkin, and B.D. Titov, in: *Proc. 19th Congress on Spectroscopy*, Tomsk (1983), Vol. 6, pp. 129–131.
130. A. Marzorati, W. Cario, and E. Zanzoterre, in: *Proc. Twelfth ILRC*, Aix-en–Provance, France (1984), pp. 259–262.
131. W. Lahman, W. Staehr, C. Weitkamp, et al., in: *Proc. IGARASS* (1984), pp. 685–688.
132. W.B. Grant, J.S. Margolis, A.M. Brothers, et al., Appl. Opt. **26**, No. 15, pp. 3033–3042 (1987).
133. H. Edner, K. Fredriksson, A. Sunesson, et al., Appl. Opt. **26**, No. 16, pp. 4330–4338 (1987).
134. N. Sugimoto, M. Matsun, and Ya. Sasano, Kokuritsu Kochai Kenko Khokoku, No. 107, 31–48 (1987).
135. H. Edner, K. Fredriksson, A. Sunesson, et all. Appl. Opt. **26**, 3183–3185 (1987).
136. H. Edner, A. Sunesson, and A. Svanberg, Appl. Opt. **27**, No. 9, 704–706 (1988).
137. H.J. Kolsh, P. Rairoux, J.P. Wolf, et al., Appl. Opt. **28**, No. 11, 2052–2056 (1989).
138. H. Edner, P. Rairoux, J.P. Wolf, et al., Appl. Opt. **28**, 921–930 (1989).
139. J.A. Sunesson and D.P. Swart, in: *Proc. Fifteenth ILRC*, Tomsk, Russia (1990), pp. 270–272.
140. A. Clerioeff, B. Calpini, et al., in: *Proc. Int. Symp. on Envir. Sensing,* Berlin, Germany (1992), pp. 343–344.
141. M.J.T. Milton, P.T. Woods, et al., Appl. Phys. **B55**, 41–45 (1992).
142. W.S. Heps and T.J. McGee, in: *Proc. Optical and Laser Remote Sensing*, ed. D.K. Kilinger (1983), pp. 167–169.
143. E.V. Browell, A.F. Carter, S.T. Shipley, et al., Appl. Opt. **22**, No. 4, 522–534 (1983).
144. T. Itabe, K. Asai, M. Ishizu, et al., Appl. Opt. **28**, No. 5, 931–934 (1989).
145. E.V. Browell, Optics Photonics News, No. 10, 8–11 (1991).
146. N.B. Nilsen, E. Uthe, and J.M. Livingston, in: *Proc. Int. Conf. Lasers* (1991), pp. 214–215.
147. R.M. Hoff, R.E. Miokle, and F.A. Froude, ASAE Transact. **32**, 1523–1528 (1989).
148. E.V. Browell, Proc. IEEE. **77**, 419–432 (1989).
149. E.V. Browell, S.T. Shipley, A.F. Carter, et al., Proc. NASA Conf. Publ., No. 2288, 6099 (1982).
150. D. Diebel, M. Bristow, and R. Zimmerman, Appl. Opt. **30**, 626 (1991).
151. A.F. Carter, E.V. Browell, and C.F. Butler, Proc. NASA Conf. Publ., No. 2288, 34–36 (1982).
152. W. Wiesemann, R. Beck, W. Englisch, et al., Appl. Opt. **15**, 257–260 (1978).
153. G. Ehret, W. Renger, and A. Schmitz–Pfieffer, in: *Proc. NCAR. NOAA. AMS*, Boulder, USA (1988), pp. 193–195.
154. D.K. Killinger and N. Menyuk, IEEE Quant. Electr. **QE–17**, No. 9, 1917–1929 (1981).
155. G. Megie, P. Flamant, M. Bourdef, et al., in: *Proc. ESA Workshop on Space Laser Appl. and Techn.* (1984), SP–202, pp. 189–195.
156. W.R. Vaughan, E.V. Browell, and W.M. Hall, in: *Proc. Fifteenth ILRC*, Tomsk, Russia (1990), Vol. 2, pp. 409–412.
157. A.V. El'nikov,V.V. Zuev, M.Yu. Kataev, et al, Atmos. Oceanic Opt. **5**, No. 6, 362–369 (1992).
158. V.V. Zuev, S.L. Bondarenko, V.D. Burlakov, et al., in: *Proc. Seventeenth ILRC*, Sendai, Japan (1994), pp. 229–230.
159. C. Cahen and G. Megie, J. Quant. Spectrosc. Radiat. Transfer **25**, 151 (1981).
160. K. Fredriksson and H. Hertz, NASA Conf. Public., No. 2288, 47 (1982).
161. J. Werner, K.W. Rote, and H. Walther, Appl. Phys. **32**. 113–118 (1983).